J Multidisciplinary Scientific Journal

Article

On the Thermal Dynamics of Metallic and Superconducting Wires. Bifurcations, Quench, the Destruction of Bistability and Temperature Blowup

Rizos N. Krikkis

Institute of Thermal Research, 2 Kanigos Str., P.O. Box 106 77 Athens, Greece; rkrik@uth.gr

Abstract: In the present study, a numerical bifurcation analysis is carried out in order to investigate the multiplicity and the thermal runaway features of metallic and superconducting wires in a unified framework. The analysis reveals that the electrical resistance, combined with the boiling curve, are the dominant factors shaping the conditions of bistability—which result in a quenching process—and the conditions of multistability—which may lead to a temperature blowup in the wire. An interesting finding of the theoretical analysis is that, for the case of multistability, there are two ways that a thermal runaway may be triggered. One is associated with a high current value ("normal" runaway) whereas the other one is associated with a lower current value ("premature" runaway), as has been experimentally observed with certain types of superconducting magnets. Moreover, the results of the bifurcation analysis suggest that a static criterion of a warm or a cold thermal wave propagation may be established based on the limit points obtained.

Keywords: superconductor stability; metallic wire; boiling; bifurcation analysis; thermal wave fronts; thermal runaway temperature blow-up

Citation: Krikkis, R.N. On the Thermal Dynamics of Metallic and Superconducting Wires. Bifurcations, Quench, the Destruction of Bistability and Temperature Blowup. *J* **2021**, *4*, 803–823. https://doi.org/10.3390/j4040055

Academic Editor: Neel Haldolaarachchige

Received: 17 October 2021
Accepted: 15 November 2021
Published: 22 November 2021

1. Introduction

Superconducting coils/magnets that produce strong magnetic fields are in high demand in contemporary cutting edge technologies such as MRI machines used in hospitals, fusion reactors, NMR spectrometers and particle accelerators, to name a few [1–3]. Although the zero resistance these coils/magnets provide is definitely very attractive, it is not free of problems, with stabilization being among the most critical. Indeed practical superconductors are susceptible to losing their superconducting ability after an increase in temperature due to disturbances (i.e., a flux jump, conductor motion or temperature rise of the boiling liquid coolant) close to the critical temperature—in which case a normal conducting mode (quenching) is formed, where the resistance increases rapidly, causing a destabilizing thermal process due to Joule heating. The concepts of the minimum length of a normal zone and the minimum quench energy of a disturbance required for the growth of a normal zone have been introduced in the analysis of the stability of superconductors [4–12]. Yet stability is not the only technological problem thus far encountered. Maeda and Yanagisawa, in their review paper [13], described the difficulty in protecting the magnet in the case of an abrupt thermal runaway as a technological challenge for the further development of high temperature superconducting coils. Thermal runaway is believed to be the reason for the electric faults in the 13kA circuits of the Large Hadron Collider in 2008, according to Werweij [14] and Willering et al. [15]. Similar behavior has been encountered in superconducting devices, where during several experiments it was observed that the quenching to a normal state of high temperature superconducting wires, tapes or films was followed by the sample's local destruction due to overheating, as reported by Rakhmanov et al. [16] and Romanovskii and Watanabe [17]. Recently, Yanagisawa et al. [18] described a method for suppressing a catastrophic thermal runaway of a REBCO coil of an NMR magnet. Furthermore, recent advances in superconducting transistors (Rocci et al. [19,20]) suggest that the non-linear, and especially the non-monotonic, temperature dependence of the resistance observed may result in an even more complicated bifurcation pattern, including limit cycles (Hopf bifurcation), as demonstrated by Elmer [21].

The stability of superconducting wires and the propagation of evaporating fronts on electrically heated metallic wires share many common features, since they are both cooled by a multi-boiling liquid and the heat generation mechanism is due to the current flow. The latter has received considerable attention after the experimental work of Nukiyama [22]. A thin metallic wire may be used as the heating and sensing element at the same time, and observations are even further facilitated, since the boiling phenomena take place exclusively along the longitudinal axis. There is a considerable literature dealing with boiling on wires. For example, Zhukov et al. [23,24] investigated the propagation of boiling modes both theoretically and experimentally. A linear approximation of the boiling heat transfer coefficient in the nucleate and film regimes, with an abrupt transition, was utilized, which resulted in an analytical expression of the wave velocity. The experiments were carried out with a platinum wire of 100 µm diameter in distilled water for various orientations of the heating element and different degrees of subcooling. The complicated structure of the nonuniform temperature field associated with the simultaneous presence of all the boiling modes appearing on heat generating elements immersed in boiling liquid has been addressed by Zhukov and Barelko [25]. Extensive experiments carried out using electrically heated thin metallic filaments, controlling either voltage, current or the element's resistance, have shown that different nonuniform modes occur on the heated surface. Moreover, estimates of the critical heat fluxes have also been given, together with a thorough discussion of the uncertainties associated with the unstable region of the boiling curve. Lee and Lu [26] investigated two-mode boiling on a horizontally heated wire for a variety of boiling liquids and wire metals. A method for calculating the equilibrium current and transition velocity was presented. Multiplicity and stability features of an electrical wire cooled by radiation have been reported by Nivoit et al. [27].

In the present study, a numerical bifurcation analysis is carried out in order to investigate the multiplicity features and the thermal runaway of metallic and superconducting wires in a unified framework. The analysis reveals that the electrical resistance, combined with the boiling curve, are the dominant factors for shaping the conditions of bistability, which result in a quenching process or conditions of multistability that may lead to a temperature blowup in the wire. An interesting finding of the theoretical analysis is that, for the case of multistability, there are two ways a thermal runaway may be triggered. One is associated with a high current value ("normal" runaway), whereas the other is associated with a lower current value ("premature" runaway), as has been experimentally observed with certain types of superconducting magnets. Moreover, the results of the bifurcation analysis suggest that a static criterion of a warm or cold thermal wave propagation may be established based on the limit points obtained.

2. Analysis

The one dimensional energy balance on a wire cooled by a multi-boiling fluid takes the form:

$$\gamma C A \frac{\partial T}{\partial t} = \frac{\partial}{\partial X}\left(KA\frac{\partial T}{\partial X}\right) - PH(T - T_\infty) + Aq_g \tag{1}$$

with Neumann boundary conditions:

$$\left.\frac{\partial T}{\partial X}\right|_{X=0} = \left.\frac{\partial T}{\partial X}\right|_{X=L} = 0 \tag{2}$$

A is the cross sectional area, P is the perimeter, γ is the density, C is the heat capacity, K is the thermal conductivity, q_g is the internal heat generation rate per unit volume due to the transport current and H is the boiling heat transfer coefficient. Introducing dimensionless variables:

$$x = X/L, \quad \tau = \alpha t/L^2, \quad \Theta = \frac{T - T_\infty}{T_{\mathrm{ref}} - T_\infty}, \quad h = H/H_{\mathrm{ref}}, \quad k = K/K_{\mathrm{ref}}, \quad c = C/C_{\mathrm{ref}} \tag{3}$$

the temperature distribution along the wire takes the form:

$$c\frac{\partial \Theta}{\partial \tau} = \frac{\partial}{\partial x}\left(k\frac{\partial \Theta}{\partial x}\right) - u^2(h\Theta - Q_g) \tag{4}$$

The conduction–convection parameter (CCP) is defined as:

$$u^2 = \frac{H_{\mathrm{ref}} L^2}{K_{\mathrm{ref}}(A/P)} \tag{5}$$

where $H_{\mathrm{ref}} = H(\Delta T_{\mathrm{ref}})$ denotes the heat transfer coefficient at a reference temperature difference ΔT_{ref}. ΔQ is the dimensionless net heat flux, i.e., the difference between the boiling heat flux and the internal heat generation heat flux:

$$\Delta Q = Q_c - Q_g = h_r\Theta - Q_g \tag{6}$$

2.1. Metallic Wire

The application of a DC current I produces an internal heat generation rate Metaxas [28]:

$$q_g = \hat{\rho}(I/A)^2, \tag{7}$$

where $\hat{\rho}$ is a temperature dependent electrical resistivity. The dimensionless heat generation rate may then be expressed as:

$$Q_g = G\rho(\Theta), \tag{8}$$

where the generation number G is defined as:

$$G = \frac{I^2}{AP}\left(\frac{\hat{\rho}}{H\Delta T}\right)_{\mathrm{ref}} \tag{9}$$

2.2. Steady State

Under steady state conditions, the partial differential equation, Equation (4), reduces to a second order ordinary differential equation for the temperature distribution:

$$\left(k\,\Theta'\right)' = u^2\Delta Q, \ \ 0 < x < 1, \tag{10}$$

with corresponding dimensionless boundary conditions:

$$\Theta'(0) = \Theta'(1) = 0, \tag{11}$$

where Θ'' and Θ' represent the second and the first derivatives with respect to x. It can be seen from Equation (10) that the dimensionless temperature Θ and its derivative Θ' will be a function of the wire's position and in addition will depend on the reduced current and the conduction–convection parameter. A simple, albeit generalized, boiling heat transfer coefficient based on a smoothed Heaviside function has been adopted, from Speetjens et al. [29]. In this way, the main features (i.e., the critical and minimum heat flux) of a typical boiling curve are retained and, at the same time, smooth and continuous derivatives may be obtained up to any desired order, which is an essential requirement for numerical accuracy and stability. Moreover, the analysis remains general and is not confined to a particular working fluid.

2.3. Wave Fronts

Equation (1) admits travelling wave solutions connecting two different uniform solutions of $\Delta Q = 0$. Introducing a different parameterization:

$$z = X/\sqrt{A}, \qquad \tau = \alpha t/A \tag{12}$$

since now the length of the wire is considered to be in the region $(-\infty,\ \infty)$, the energy balance takes the form:

$$c\frac{\partial \Theta}{\partial \tau} = \frac{\partial}{\partial z}\left(\frac{\partial \Theta}{\partial z}\right) - \mathrm{Bi}\Delta Q \tag{13}$$

where $\mathrm{Bi} = P(H/K)_{\mathrm{ref}}$ is the Biot number. Travelling wave solutions will be of form, $\Theta(z,\tau) = \Theta(z - v\tau)$ and substituting $\xi = z - v\tau$ in Equation (13) yields:

$$\left(k\,\Theta'\right)' + vc\,\Theta' - \mathrm{Bi}\Delta Q = 0 \tag{14}$$

The primes now denote differentiation with respect to ξ and the front profile will depend on G and Bi. The travelling wave solution is subjected to the below boundary conditions:

$$\lim_{\xi \to \pm\infty} \left(\Theta,\ \Theta'\right) = \left(\Theta_{\pm}, 0\right) \tag{15}$$

where $\Theta_{\pm}$ are two zeros of $\Delta Q = 0$.

2.4. Stability

The stability of a certain steady state $\Theta_s(x)$ to small perturbations $\vartheta(x)$, i.e.:

$$\Theta(x,\tau) = \Theta_s(x) + \vartheta(x)\exp(\lambda\tau) \tag{16}$$

is determined by the eigenvalues λ of the corresponding Sturm–Liouville problem after substituting Equation (16) into the original partial differential equation, Equations (10) and (11):

$$\left(k\vartheta'\right)' + k_{\Theta}{\Theta'}_s\vartheta' - \left[u^2\Delta Q_{\Theta} + c\lambda - k_{\Theta\Theta}{\Theta'}_{s2} - k_{\Theta}{\Theta''}_s\right]\vartheta = 0, \qquad 0 < x < 1 \tag{17}$$

with corresponding boundary conditions, $\vartheta'(0) = \vartheta'(1) = 0$. During branch tracing, for every steady state that has been calculated from Equations (10) and (11), the associated Sturm–Liouville problem, Equation (17), is subsequently numerically solved and a sufficient number of eigenvalues are determined. Stable solutions are characterized by negative eigenvalues, whereas positive eigenvalues correspond to unstable temperature distributions.

2.5. Superconducting Composite Wire

For the superconducting composite wire the usual approximation is being employed, following Bellis and Iwasa [8]. With the aid of the previous definitions, the dimensionless variables it may be expressed as below:

$$Q_g = \begin{cases} 0 & \Theta \le \Theta_{cs} \\ G\rho\frac{\Theta - \Theta_{cs}}{\Theta_c - \Theta_{cs}} & \Theta_{cs} \le \Theta \le \Theta_c \\ G\rho & \Theta \ge \Theta_c \end{cases} \tag{18}$$

where Θ_c is the critical temperature at $I = 0$ and Θ_{cs} is the temperature at which current sharing starts. The thermal conductivity and the heat capacity in Equation (4) represent average properties of the metal matrix and the superconductor since the composite structure of the wire has be taken into account. Furthermore, the generation number is defined similarly to Equation (9) as:

$$G = \frac{I^2}{fAP}\left(\frac{\hat{\rho}}{H\Delta T}\right)_{\mathrm{ref}} \tag{19}$$

3. Results, Applications and Discussion

The second order, two-point boundary value problem described by Equations (10) and (11) has been solved numerically. Continuation along the various branches has been carried out along the lines suggested by Seydel [30]. For the computation of the singular points, an extended problem is formed by the partial derivatives of Equations (10) and (11) with respect to the parameters, according to Witmer et al. [31]. The continuous and smooth boiling curve enables the numerical calculation of both monotonic and oscillating fronts from the boundary value problem of Equation (14). Practically, we are seeking a truncated heteroclinic orbit on a finite interval, since it will take an infinite amount of time for a particle to follow the ideal trajectory moving from one uniform solution to the other. Since the heteroclinic orbit enters or leaves the uniform solutions tangentially to the eigenspaces, the truncated orbit should start and end close to the corresponding eigenspaces related to the saddles $\Theta_{\pm}$. Thus, certain free parameters are introduced that measure the distances of the starting and ending points of the approximate orbit with respect to the saddles, following Beyn [32] and Friedman and Doedel [33]. In this way, an extended boundary value problem is solved for the determination of the wave profile and its speed. Because the problem is by no means trivial, and in order to avoid spurious wave fronts, an additional solution methodology is applied. The integration is started close to the unstable manifold of Θ_{-} from the left side of the interval and close to the stable manifold of Θ_{+} from the right side of the interval, matching the temperature and its first and second derivatives from each side at an interior point, say $\xi = 0$. The continuity of the wave profile at the matching points provides three nonlinear algebraic equations by which the wave speed and the temperature at the edges of the interval are determined.

3.1. Metallic Wires

The problem of a boiling wire is very similar to the problem of boiling on extended surfaces (fins) with internal heat generation and flat plates (Krikkis [34,35]), with the notable exception of the boundary conditions; i.e., only the heat dissipation from the wire's surface area is important and the tips are assumed to be insulated. Again, a very large number of solutions exist, as is depicted in Figure 1, in which the projection of the singular points (limit points and pitchfork bifurcation points, as will be explained next) on the (u, G) plane is shown. The boundary conditions have a profound effect, since the solution structure is radically different compared to the nested cusp points calculated for the boiling fin case [34]. Multiple steady states are confined within specific values of the generation number G, and as the conduction-convection parameter increases the number of solutions increases as well. Up to nine multiple solutions are calculated in Figure 1. For the particular boiling flux and electrical load curves under consideration, the multiple solutions are contained within a range of generation number values with a lower limit of $G \approx 0.25$ and an upper limit of ≈ 0.99. This may be explained in terms of the behavior of the uniform solutions of Equation (10), i.e., $\Theta' = \Theta'' = 0$, $\Theta(x) = \text{const}$, determined by the zeros of the net heat flux:

$$\Delta Q = Q_c(\Theta) - Q_g(\Theta, G) = 0 \tag{20}$$

which are graphically depicted in Figure 2. As long as the generation curve $Q_g(\Theta, G)$ remains below the minimum heat flux point M_2 $\Theta = 1.62$, $Q_c = 0.25$, only one intersection point between Q_g and Q_c exists, say Θ_{u1}, and Equation (10) has one solution. Similarly, when Q_g lies above the critical heat flux point M_2 $(\Theta = 0.60,\ Q_c = 1.00)$, only one intersection point Θ_{u3} exists and consequently a unique solution exists. For intermediate values of the generation number, three uniform solutions exist: Θ_{u1}, Θ_{u2} and Θ_{u3}. It should be pointed out that even if Equation (20) has three solutions, Equation (10) may have more solutions as u increases because of the diffusion term in Equation (10).

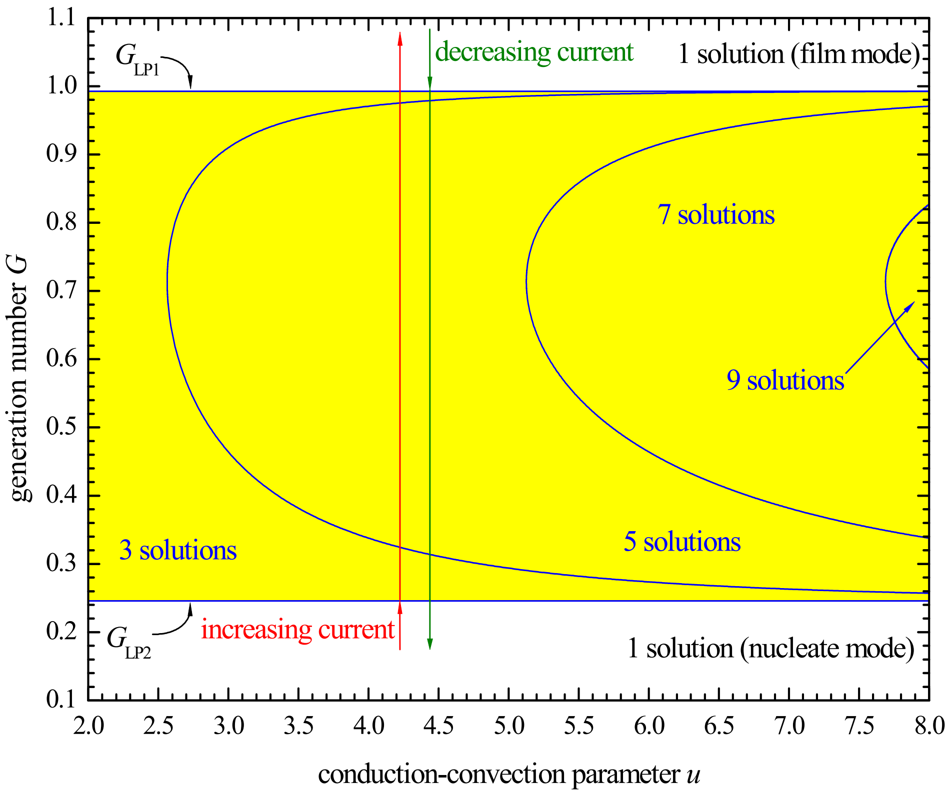

Figure 1. Projection of the singular points on the (u, G) plane.

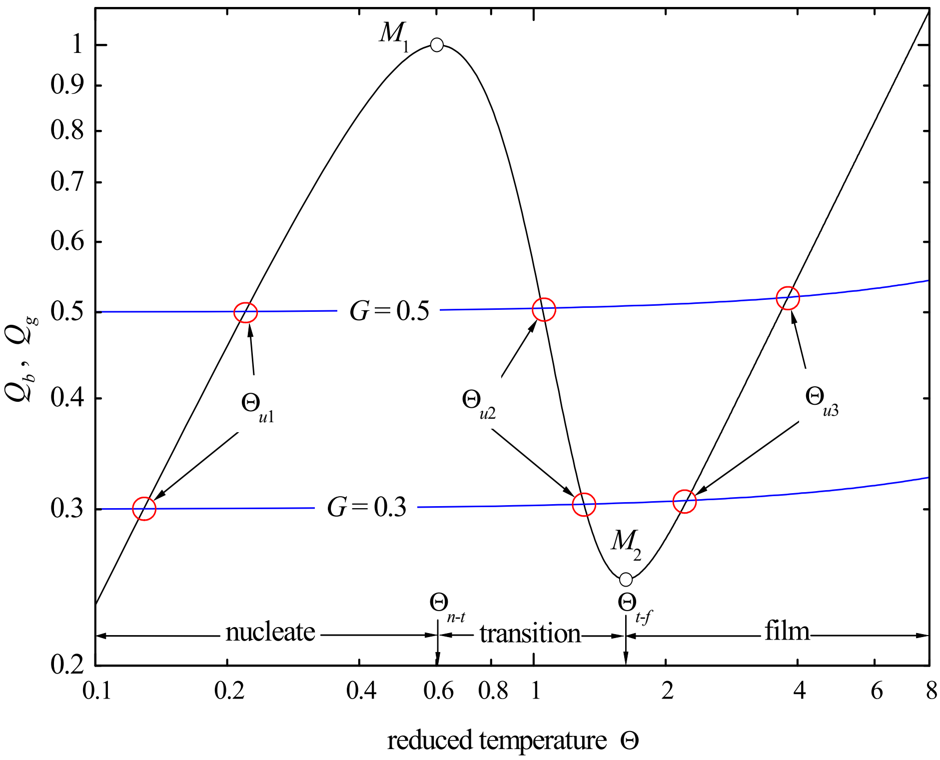

Figure 2. Uniform solutions $\Delta Q = Q_c(\Theta) - G\rho(\Theta) = 0$.

In order to describe the solution structure, $\Theta_e = \Theta(0)$ is selected as a measure of $\Theta(x)$. The corresponding bifurcation diagram is an S-shaped curve and is presented in Figure 3 for $u = 1$. Up to three uniform solutions exist, corresponding to the three boiling modes—nucleate (stable), transition (unstable) and film (stable)—which are marked with a continuous and dashed line accordingly. Two limit points calculated from the below relationship:

$$(\partial\Theta_e/\partial G)_u = 0 \tag{21}$$

separate the stable and unstable branches. As CCP is increasing, the number of multiple solutions increases and the solution pattern becomes more complex, as shown in Figure 4. For $u = 3$, a separate (and unstable, as it will be shown later) closed branch appears, which emanates from the intermediate unstable transition boiling branch through two pitchfork bifurcation points. A further increase to the CCP results in additional nonintersecting nested branches, as presented in Figure 5. It is worth mentioning that this structure is very similar to the one calculated by Speetjens et al. [29] for a two dimensional thick plane heater in pool boiling. The projection of the limit points and the pitchfork bifurcation points on the (u, G) plane is the abstract result presented in Figure 1.

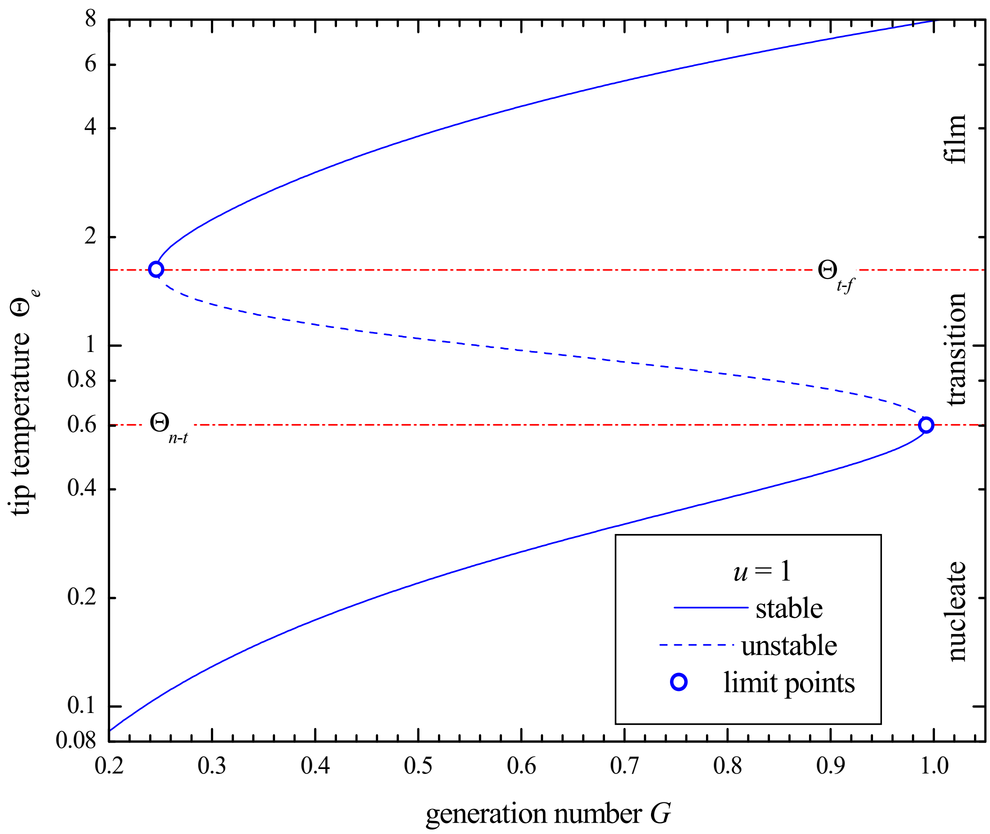

Figure 3. Solution structure for a wire with $u = 1$.

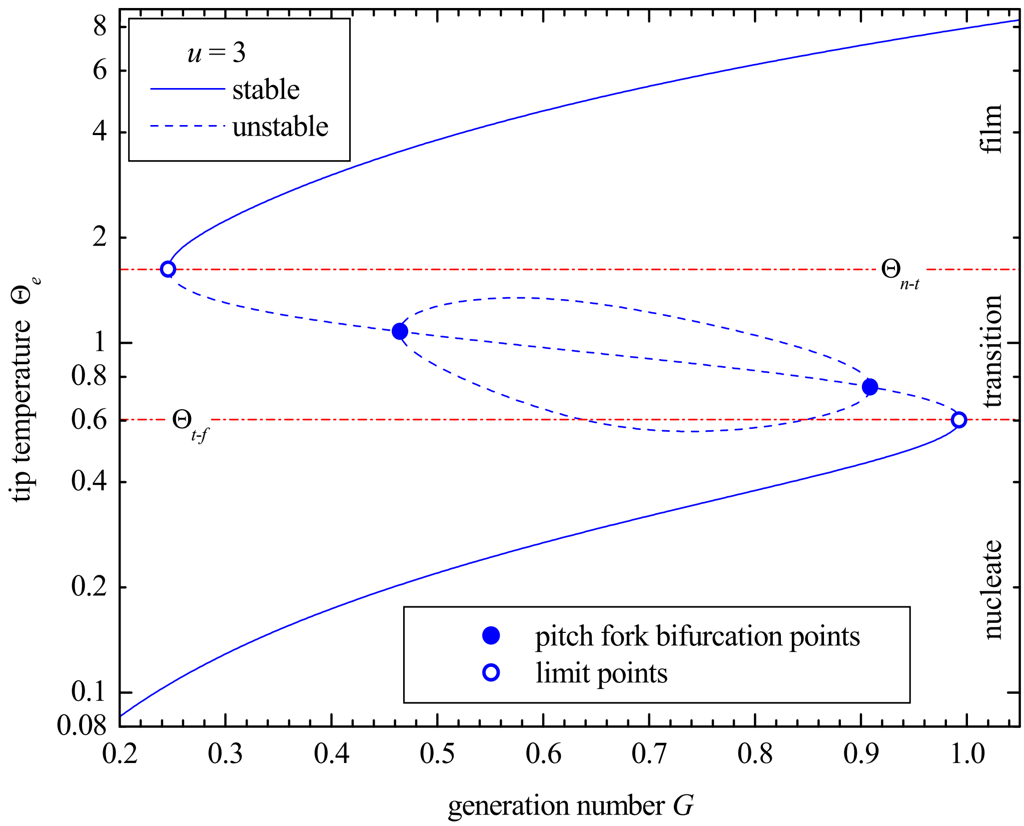

Figure 4. Solution structure for a wire with $u = 3$.

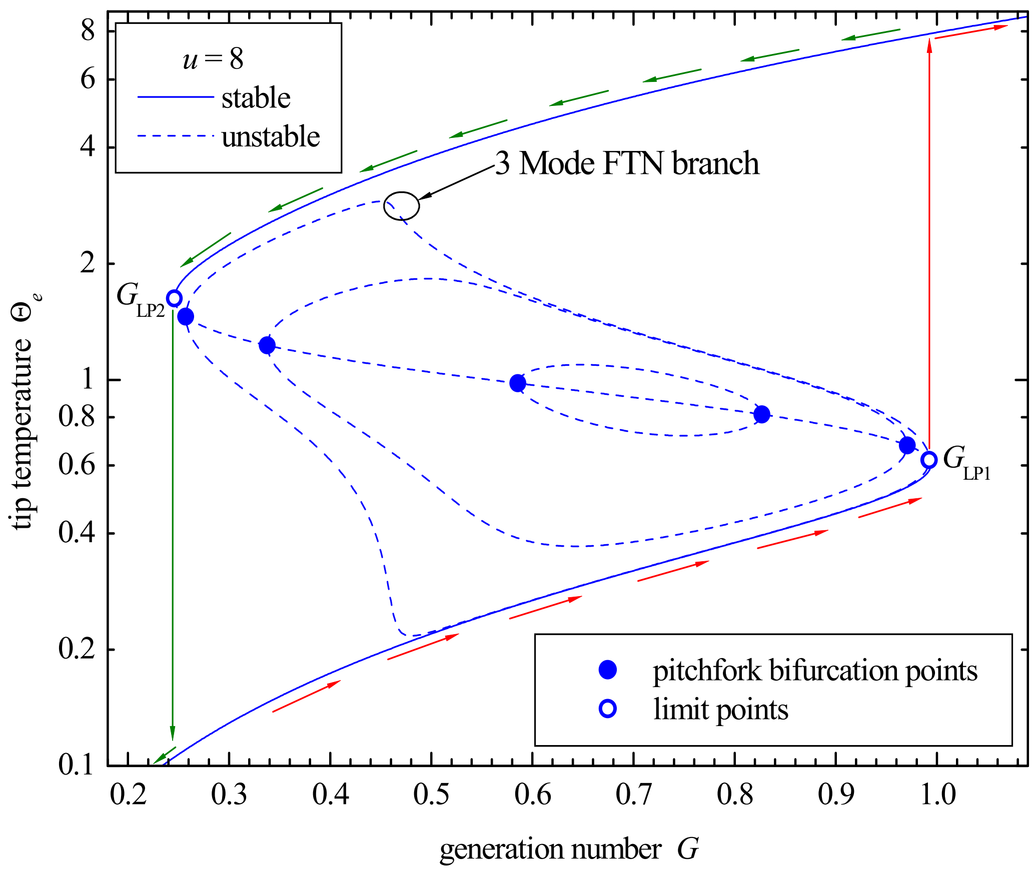

Figure 5. Solution structure for a wire with $u = 8$.

Seven out of the total nine temperature distributions along the wire's length are demonstrated in Figure 6 for $G = 0.46$ and $u = 8$ (the smallest index is associated with the smallest tip temperature), which are in qualitative agreement with the ones calculated by Kovalev and Usatikov [36] for water. In addition to the three uniform solutions $\Theta_1(x) = \Theta_{u1}$, $\Theta_4(x) = \Theta_{u2}$ and $\Theta_7(x) = \Theta_{u3}$, symmetric (with respect to $x = 0.5$) non-uniform solutions in the form of standing waves exist, Θ_3 and Θ_5, together with antisymmetric ones, i.e., Θ_2 and Θ_6. Of particular interest are the solutions in which all three modes (film, transition and nucleate FTN) are simultaneously present along the wire length: i.e., temperature distributions Θ_2 and Θ_6. This coincidence is indicated in Figure 7 for the solution $\Theta_2(x)$, where, as the conduction–convection parameter u increases, the wire tip is almost attached to the uniform temperature Θ_{u1}, corresponding to the nucleate mode, whereas the base temperature is close to Θ_{u3}, which corresponds to the film mode. Moreover, with increasing u the nucleate regime gradually displaces the film regime and the transition zone becomes shorter (i.e., its length is inversely proportional to the CCP). The terminal characteristics of the wire may be obtained from Ohm's law:

$$\hat{\rho} j = \frac{d\Phi}{dX} \tag{22}$$

where Φ is the electric potential. Utilizing the dimensionless variables in Equation (3) and introducing a dimensionless electric potential $\phi = \Phi/\Phi_{\mathrm{ref}}$ with $\Phi^2_{ref} = (\hat{\rho} K \Delta T)_{\mathrm{ref}}$, the voltage drop across the wire is then obtained by integrating Equation (22) along the wire for the temperature profiles that have already been calculated from the solution of Equations (10) and (11):

$$\Delta\phi = u\sqrt{G} \int_0^1 \rho(\Theta) dx \tag{23}$$

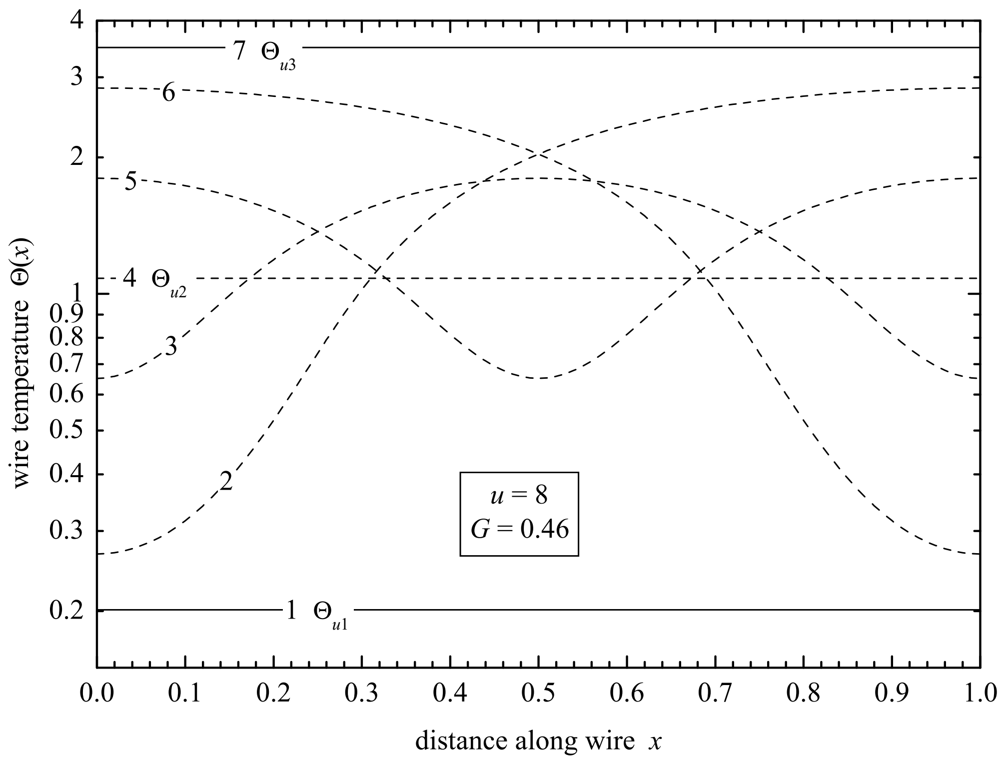

Figure 6. Wire temperature distributions for $G = 0.46$ and $u = 8$.

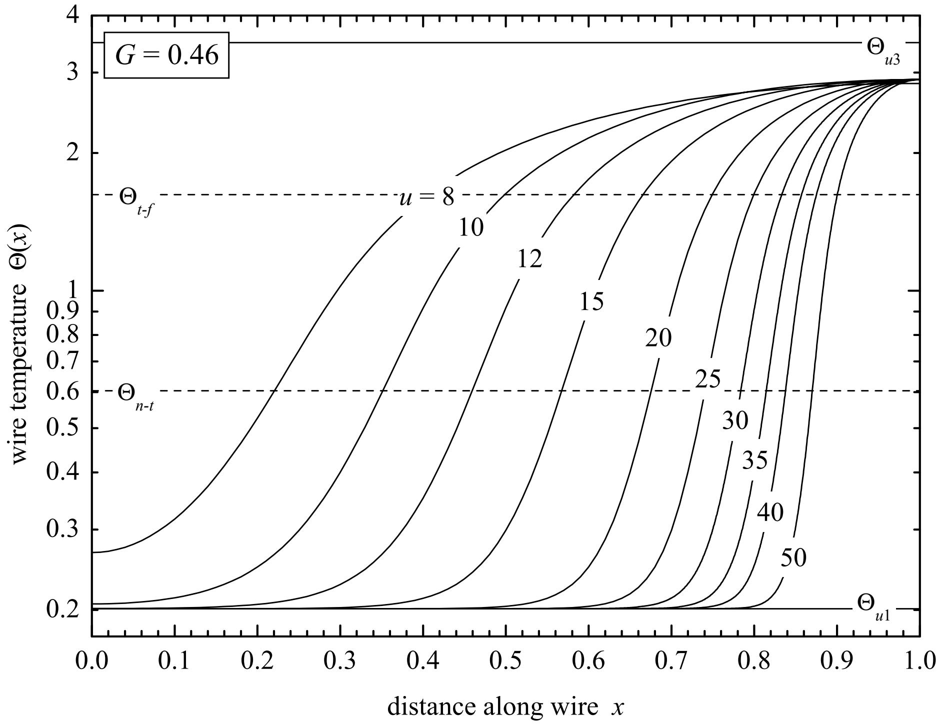

Figure 7. Wire temperature profiles $\Theta_2(x)$ as a function of u for $G = 0.46$.

The results are depicted in Figure 8 for $u = 3$ and are in qualitative agreement with the measurements taken by Zhukov and Barelko [25], presented as an insert in the same figure for convenience. Because of the integral in Equation (23), the two antisymmetric solutions collapse onto a single curve; i.e., the wire resistance will be same.

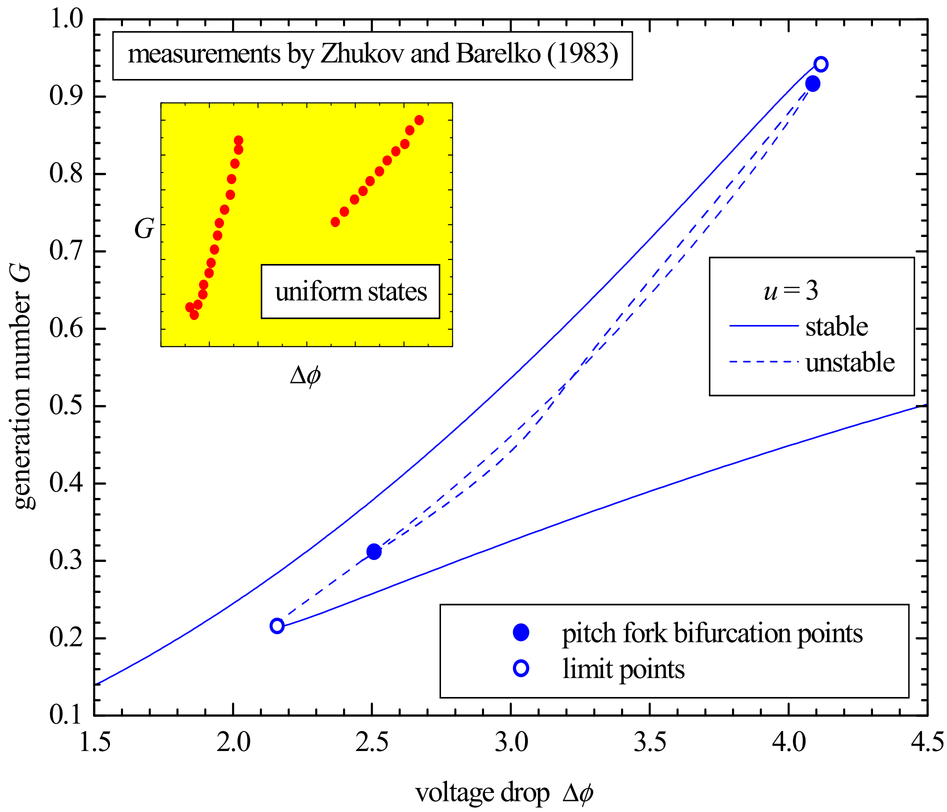

Figure 8. Terminal characteristics for $i =$ const and $u = 3$.

3.2. Quench, the Destruction of Bistability and Thermal Runaway

The combination of the high temperatures involved in the film boiling regime with a particular wire resistance curve is depicted in Figure 9. In such a case, as the temperature increases the gradient of the electrical current flux will exceed the gradient of the boiling curve and a fourth (unstable) intersection point will appear; i.e the equation $\Delta Q = 0$ has four zeros. The solution structure for low to moderate temperatures, say $\Theta_e < 2$, appears to be similar to the case with three uniform solutions; however, the length of the upper stable branch is significantly reduced and an additional limit point appears, followed by an unstable branch at higher temperatures, as shown in Figure 10. At this point, it is interesting to return to Figure 5 and discuss the mechanism of transition between two stable solutions. Assuming that the wire is operating at the nucleate regime, as the applied current increases the operating point moves along the red arrows. As soon as the current exceeds the value of the low temperature limit point, i.e., $G > G_{\text{LP1}}$, the operating point will jump to the upper branch of the stable film boiling regime through a wave front mechanism described in Section 2.3; i.e., a warm (film) zone (or mode) will propagate along the wire axis and replace the prevailing cold one (nucleate). This mechanism is also referred to as an autowave by Zhukov et al. [23,24] and a switching wave by Gurevich and Mints [7]. Similarly, when the wire is operating in the film boiling regime and the applied current is decreasing, the operating point will move along the direction of the green arrows up to the high temperature limit point. With further reduction of the current below the limit point, $G < G_{\text{LP2}}$, a low temperature (nucleate) operating point will be established, as the wave front will gradually replace the film boiling mode by the nucleate one. Thus, from the practical point of view the two limit points represent a static criterion of a warm zone propagation if the generation number exceeds the low temperature limit point, and a cold zone propagation if the generation number is reduced below the high temperature limit point. The propagation of zones may be also represented with the aid of Figure 1, where the limit points G_{LP2} and G_{LP1} define the multiplicity area. Following a vertical path of constant conduction–convection parameter u for increasing or decreasing current, the state of the system will change from film to nucleate boiling (or vice versa) as soon as the corresponding limit points are encountered.

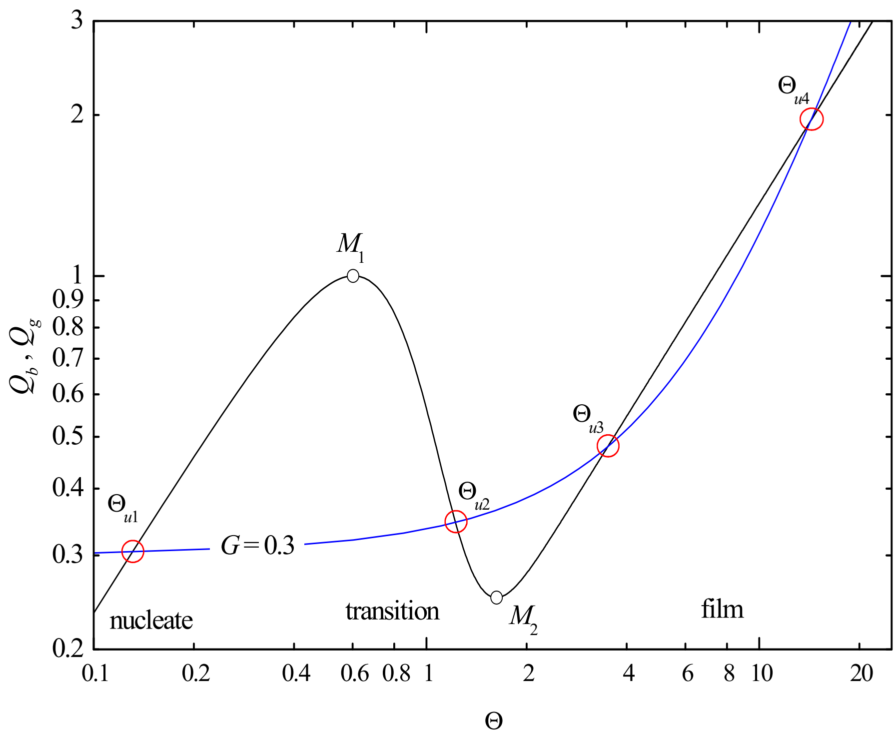

Figure 9. Example of four solutions of $\Delta Q = Q_c(\Theta) - G\rho(\Theta) = 0$.

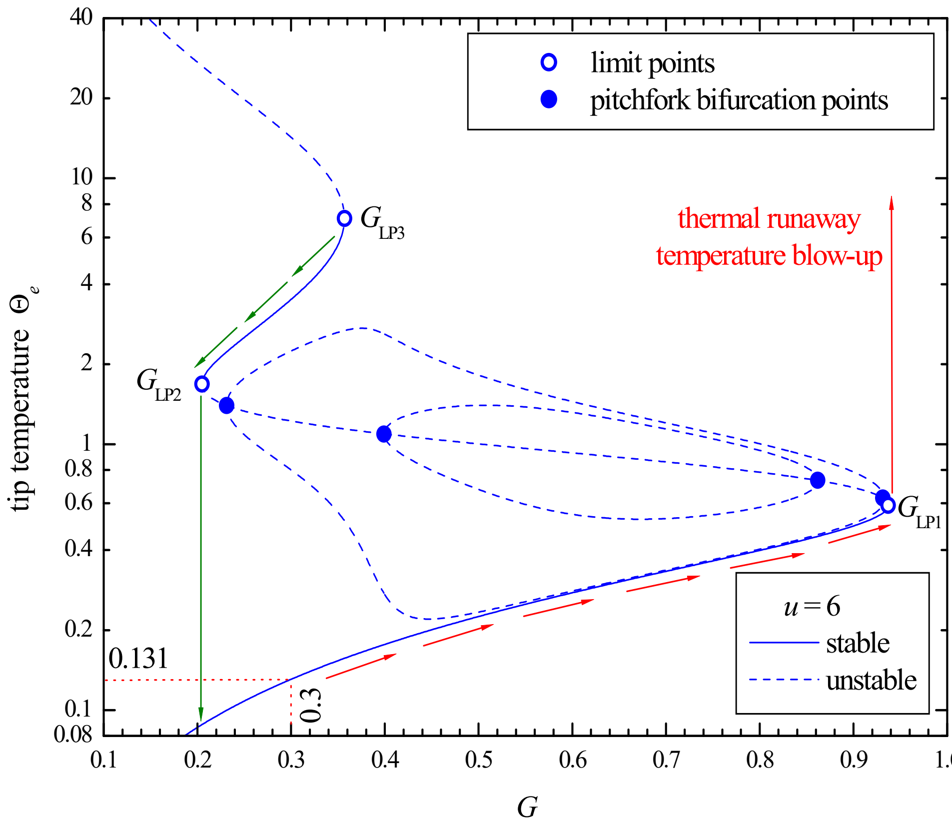

Figure 10. Solution structure at higher temperatures and thermal runaway.

Now, a closer look at Figure 10 reveals that no such switching mechanism exists between the stable states. Indeed, starting from an operating point in the nucleate regime, as the current increases the wire temperature will follow the red arrows up to the limit point. However, beyond the lower temperature limit point, that is, for $G > G_{\mathrm{LP1}}$, no solution exists. This is of paramount practical importance, because if the operating current during a transition or fault exceeds this limit point, Equation (4) can exhibit unbounded growth in a finite time—that is, a thermal runaway or temperature blow-up. This phenomenon has been discussed qualitatively by Gurevich and Mints [7] and rigorously by Bandle and Brunner [37]. An engineering application for current leads for superconducting magnets has been presented by Krikkis [38]. In that case, however, the solution structure is much simpler, since only two solutions exist. This is because the heat dissipated by the conduction and boiling can no longer match the heat generation rate produced by the applied current (Joule heating). It is worth mentioning that the thermal runaway is also encountered in everyday life, when for instance, in a common switchboard during a short-circuit (i.e., an overcurrent) a fuse or even a group of cables may be burnt out before the safety relays are activated. Therefore for such a combination of boiling curve and wire electrical resistivity, the low temperature limit point G_{LP1} is also the threshold for thermal runaway. This is better demonstrated with the numerical blow-up solution of Equation (4) shown in Figure 11. Starting from a uniform steady state with $G(\tau = 0) = 0.3$ and $\Theta(x, \tau = 0) = 0.131$, the generation number $G(\tau)$ is subjected to a step-like change (see the insert in Figure 11). It is worth noticing that during the transition the temperature profile remains uniform in x. As soon as the lower limit point $G_{\mathrm{LP1}} = 0.937$ is exceeded, the unbounded growth in the temperature is clearly evident in Figure 11. Another feature of the smooth and continuous boiling curve worth mentioning is that it enables the numerical calculation of the monotonic (stable) and oscillating (unstable) wave fronts that connect the various uniform steady states, as shown in Figures 12 and 13, respectively. A notation similar to that used by Dabholkar et al. [39] has been adopted in the description of the fronts; i.e., v_{12} refers to the travelling wave speed connecting uniform states 1 and 2.

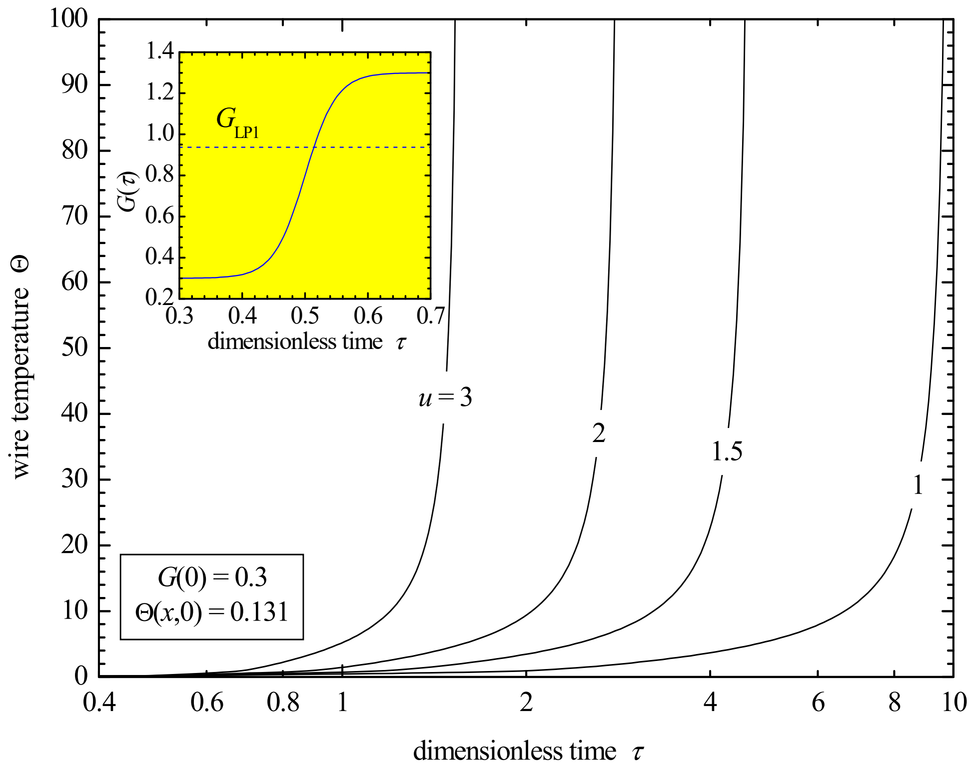

Figure 11. Temperature blow-up for a step-like change in the generation number.

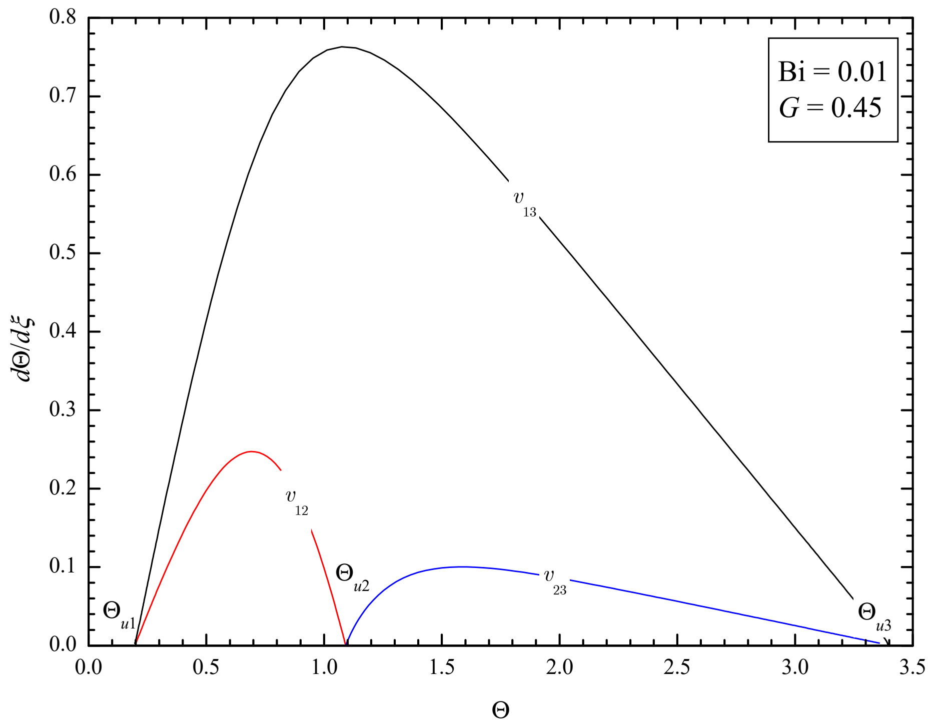

Figure 12. Monotonic wave fronts.

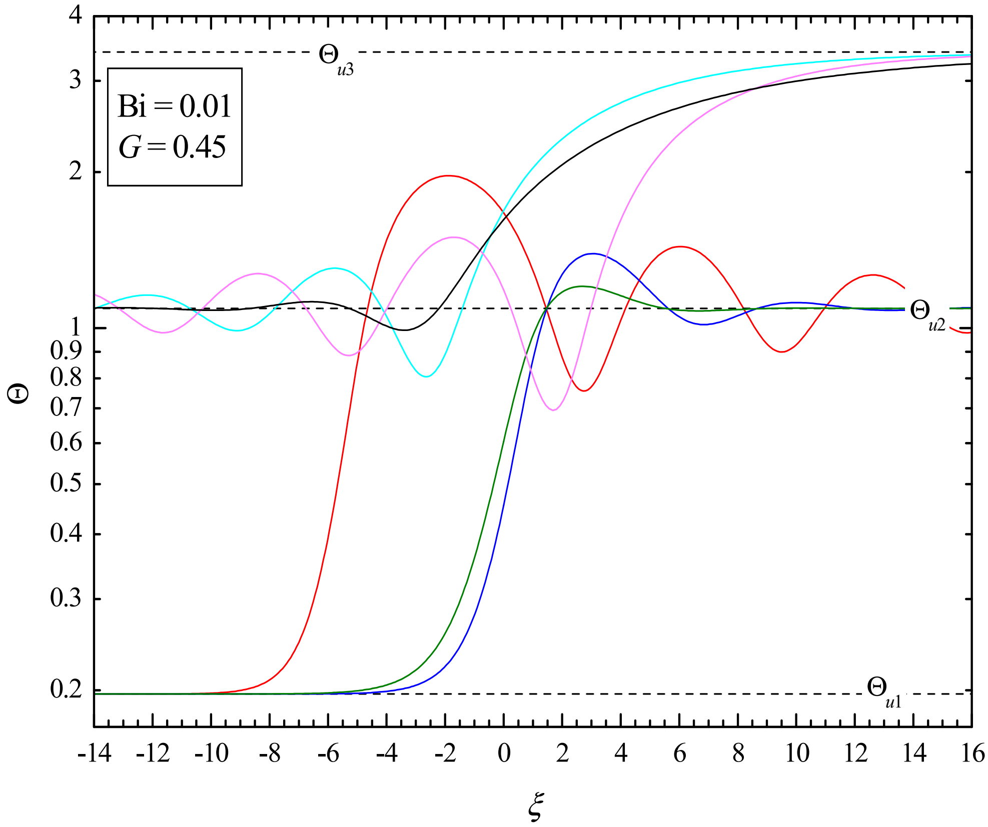

Figure 13. Oscillating wave fronts.

3.3. Stability

Stable solutions are designated with a continuous line and unstable solutions with dashed lines in the relevant diagrams. Solutions emanating from the transition boiling regime and belonging to the inner branches are highly unstable, since they are associated with two positive eigenvalues. Two uniform stable solutions corresponding to the film and nucleate boiling modes have been calculated, while the remaining ones are unstable. The instability of all the non-uniform states for an exactly solvable, closely related problem has been proved by Bedeaux and Mazur [40] (and the references therein). The convective heat transfer coefficient was assumed to be temperature independent, whereas the conductor's resistivity was modeled as a step function between zero and finite resistance, representing the superconducting and the normal state, respectively. Elegant proofs of the instability of standing wave solutions to a similar problem regarding simultaneous heat and mass transfer on a wire have been presented by Luss and Ervin [41], based on topological arguments, and by Jackson [42], who employed Sturmian theory for ordinary differential equations. Epitomizing the performance of the model, consistent temperature profiles and terminal (voltage–current) characteristics as compared with the experimental measurements may be obtained. Moreover both monotonic and oscillating wave front solutions may be calculated. Arguing on such grounds, it is reasonable to conclude that the stability features are consistent as well. However, in such a case, how does one reconcile the stability results with the experimentally observed multi-boiling modes? The answer appears to lie in recognizing the profound effect of the CCP on the positive eigenvalue, which is responsible for the instability. Referring to Figure 14, the eigenfunction expansion of an FTN mode (i.e., solutions Θ_2 and Θ_6 in Figure 6) and in particular the magnitude of the of the positive eigenvalue, say λ_1, has been calculated as a function of the generation number and the CCP. As u is increases, there is a substantial reduction in the magnitude of λ_1 (roughly two orders of magnitude) in a very confined zone around $G \cong 0.45$ (i.e., a "deep well") that is related to the so called "equilibrium current". For a typical wire of length 100 mm and diameter 1 mm used in experiments, $u > 10$, as λ_1 approaches zero it will take a long time before the exponential term in Equation (16) becomes significant, and the solution may be physically realizable before it is destabilized. Consequently, only the uniform solutions are stable, in contrast to the stable multi-mode boiling on fins.

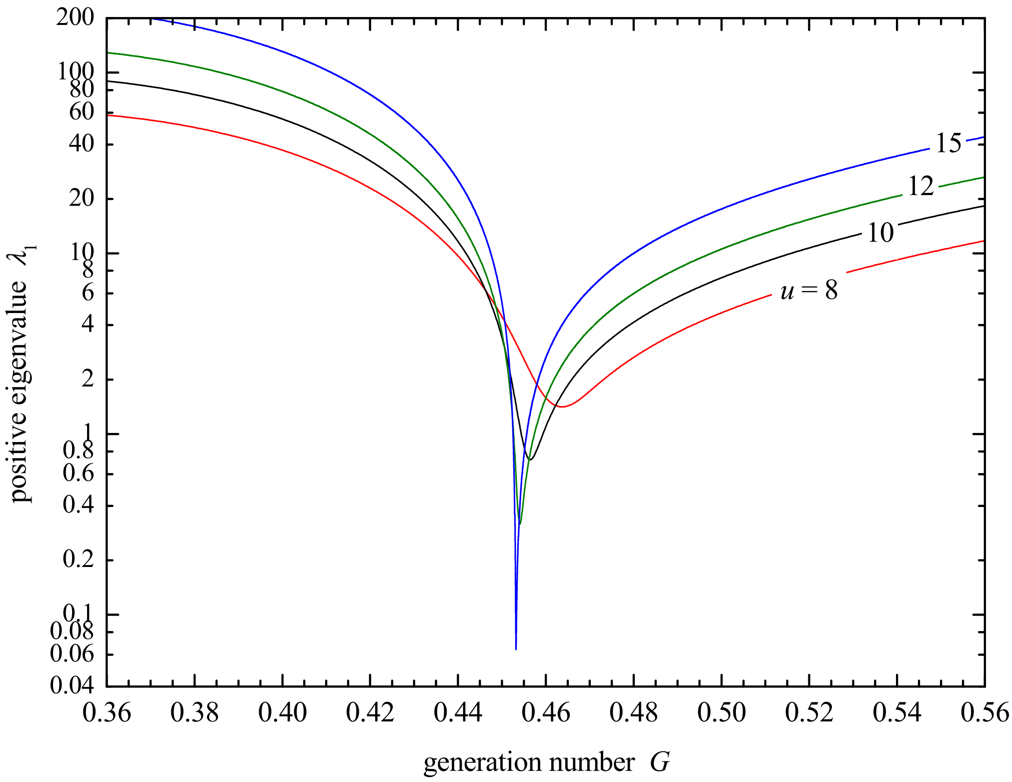

Figure 14. The positive eigenvalue λ_1 as a function of u.

3.4. Superconducting Composites

The case of superconducting wire is quite similar to the case of metallic wire, and the results are summarized in Figure 15. When three uniform solutions exist, as in Figure 15a, the steady state solutions are bistable. Two stable and uniform solutions corresponding to the nucleate and film boiling regimes exist among several unstable steady states. The number of the unstable states depends on the value of the CCP. Starting from the lower stable branch and gradually increasing the current (along the red arrows in Figure 15b), a series of stable states may be obtained up to the limit point G_{LP1}. Beyond this point, any increase in the current will cause a jump to the upper steady state of higher temperature, resulting in a quench. No thermal runaway is possible with this solution structure.

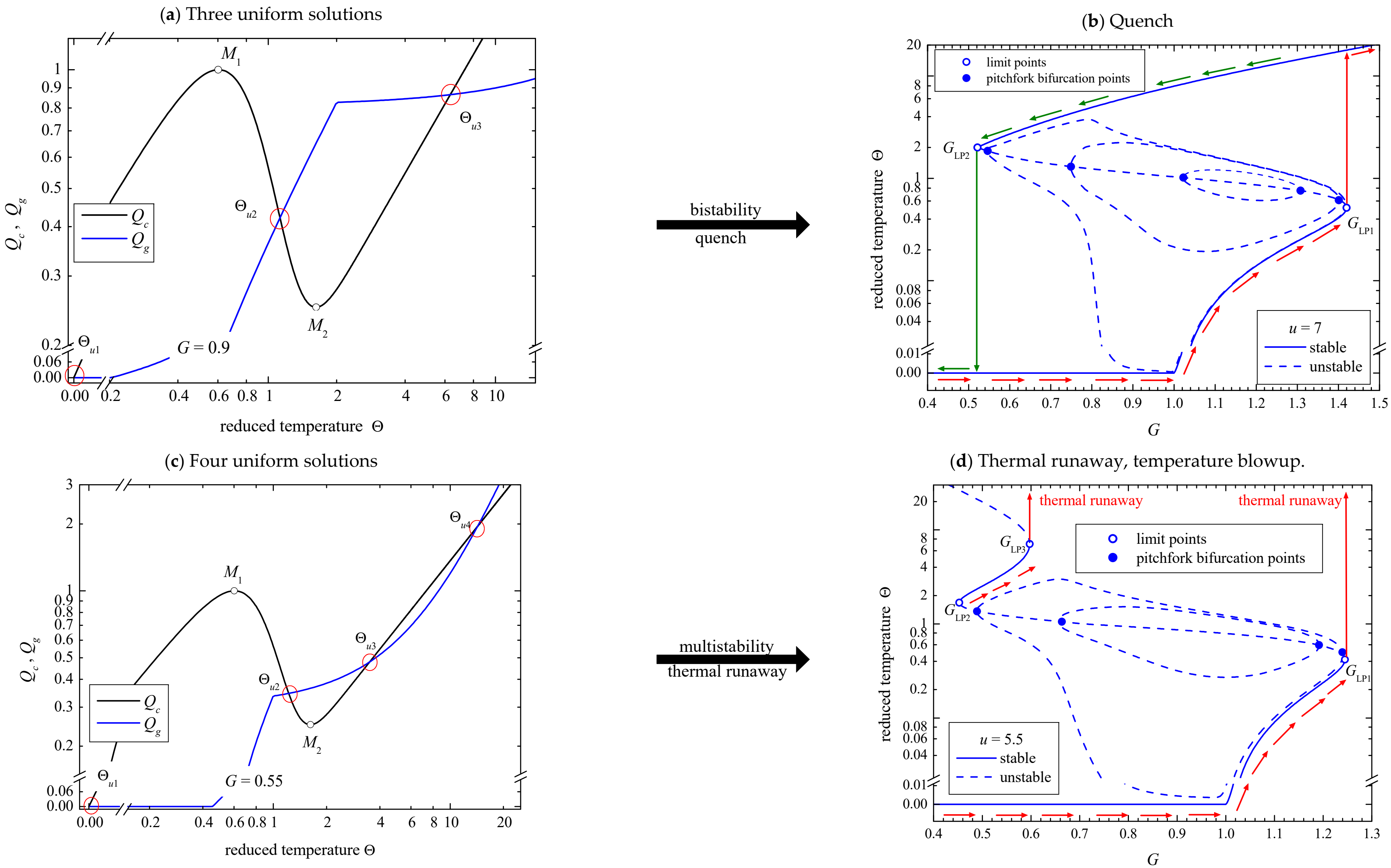

Figure 15. Superconducting composite. Quench, the destruction of bistability and thermal runaway.

As the number of uniform solutions increases from three to four, as shown in Figure 15c, the solution structure at higher temperatures changes radically, because the resistivity is a stronger function of the temperature. The stable branch observed in Figure 15b has been substantially reduced and an additional limit point, G_{LP3}, appears at a higher temperature but at a lower current. Consequently, the bistability is progressively destroyed and replaced by multistability. The solution structure imposed by the multistability is prone to thermal runaway if the applied current exceeds the values of the corresponding limit points, either on the lower or on the upper stable branches, as shown in Figure 15d. This process is referred to as "normal" runaway by Maeda and Yanagisawa [13].

Let us now try to explain the phenomenon of "premature" runaway, which has been experimentally observed by Maeda and Yanagisawa [13], within the framework of the bifurcation analysis presented thus far. For this reason, the net heat flux, Equation (20), is modified with an energy term to take into account a local disturbance:

$$\Delta Q = Q_c(\Theta) - Q_g(\Theta) - Q_d(x) \tag{24}$$

The disturbance is modeled by a cutoff Gaussian function centered at the middle of the wire, $x_m = 0.5$:

$$Q_d(x) = D \exp\left[-(x - x_m)^2/w^2\right] \tag{25}$$

where D is the disturbance strength. The effect of the disturbance on the solution structure is shown in Figure 16, where the unstable non-uniform solutions have been suppressed for clarity. As the strength of the disturbance increases, all the limit points shift in the direction of lower current. Consequently, when an operating point $G < G_{\mathrm{LP1}}$ with $Q_d = 0$ at say $\tau = 0$ has been established and a disturbance appears at $\tau > 0$ then the new limit point G_{LP1} corresponds to a lower current, and at the same time the applied current remains fixed. Under these conditions, thermal runaway is possible if the disturbance strength is sufficient to reduce G_{LP1} below the operating current value, as is schematically shown in Figure 16. The numerical solution of Equation (4) depicting this temperature blow-up is shown in the same figure as an insert. It should be pointed out that for the case without disturbance, the limit points may easily be calculated algebraically, requiring simultaneously the intersection points to be tangential contact points as well, i.e.:

$$\left.\begin{array}{l} \Delta Q = 0 \\ \frac{d\Delta Q}{d\Theta} = 0 \end{array}\right\} \tag{26}$$

When a local disturbance $Q_d(x)$ is present, no uniform solutions exist, since ΔQ is now a function of the wire's temperature and position. Therefore the limit points must be calculated from the solution of the extended boundary value problem defined by Equations (10) and (11), as was described by Seydel [30] and Witmer et al. [31].

Is the "premature" runaway predictable after all? To the extent that a quantitative description (or at least an estimate) of the disturbance is available, then as it is demonstrated in the present study, singularity theory (Golubitsky and Scaeffer [43]) may be employed for the calculation of the new limit points (i.e., Figure 16), which determine the new runaway threshold.

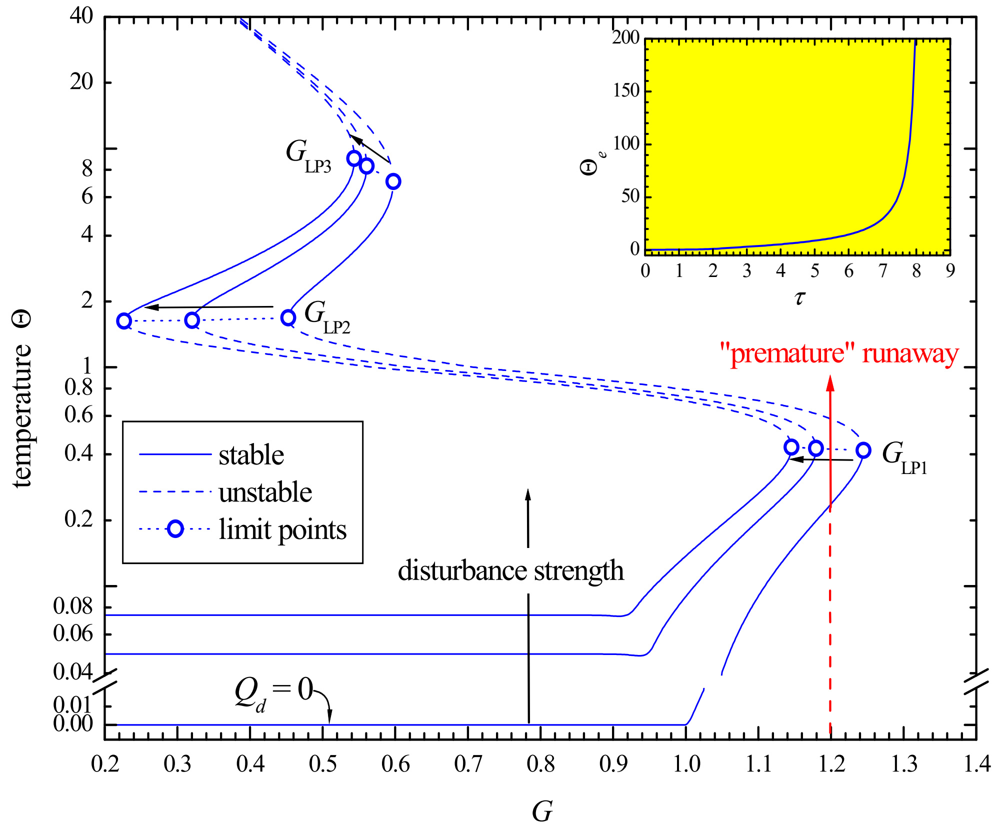

Figure 16. Effect of disturbances on the limit points and "premature" runaway explanation.

4. Conclusions

A complete picture of the solution structure is presented for metallic and superconducting wires stabilized in a multi-boiling liquid utilizing a generalized heat transfer coefficient and a one dimensional conduction-convection model with Newmann boundary conditions. Multiple steady states together with its stability characteristics, travelling wave solutions and temperature blowup have been calculated.

The conduction along the wire substantially affects the solution structure especially at higher values of the conduction-convection parameter, since more solutions may exist than the roots of the corresponding uniform states defined by $\Delta Q = 0$. For the bistability case, the two limit points corresponding to nucleate and film boiling regimes comprise a static criterion of the propagation a warm zone if the applied current exceeds the low temperature limit point, and a cold zone if the current is reduced below the high temperature limit point.

Furthermore, the analysis reveals that the electrical resistance combined with the boiling curve are the dominant factors shaping the conditions of bistability—which result in a quenching process—or the conditions of multistability—which may lead to a temperature blowup in the wire. An interesting finding of the theoretical analysis is that for the case of multistability there are two ways a thermal runaway may be triggered. One is associated with a high current value, whereas the other one is associated with a lower value, as has been experimentally observed for certain types of superconducting magnets.

Funding: This research received no external funding.

Conflicts of Interest: The author declares no conflict of interest.

Nomenclature

A	cross sectional area	[m^2]
Bi	Biot number	[-]
c	(C/C_{ref}) reduced specific heat capacity	[-]
C	specific heat capacity	[J/(kgK)]
D	disturbance strength	[-]
f	volume fraction of normal metal	[-]
G	generation number	[-]
h	(H/H_{ref}) reduced heat transfer coefficient	[-]
H	heat transfer coefficient	[W/(m^2K)]
I	applied current	[A]
j	current density	[A/m^2]
k	(K/K_{ref}) reduced thermal conductivity	[-]
K	thermal conductivity	[W/(mK)]
L	conductor length	[m]
P	perimetry	[m]
q_g	internal heat generation rate per unit volume	[W/m^3]
Q_g	reduced internal heat generation rate	[-]
Q_c	$(h_r\Theta)$ reduced boiling heat flux	[-]
t	time	[sec]
T	temperature	[K]
x	(X/L) dimensionless distance along wire	[-]
X	distance along wire	[m]
u	conduction-convection parameter	[-]
v	dimensionless front velocity	[-]
w	disturbance width parameter	[-]
z	longitudinal co-ordinate	[-]
Greek Symbols		
α	thermal diffusivity	[m^2/s]
ΔQ	$(Q_c - Q_g)$ reduced heat flux difference	[-]
ΔT	$(T - T_\infty)$ temperature difference	[K]
Θ	$[(T - T_\infty)/(T_{\mathrm{ref}} - T_\infty)]$ dimensionless temperature	[-]
Θ_c	critical temperature at $I = 0$	[-]
Θ_{cs}	temperature where current sharing starts	[-]
Θ_{n-t}	knot temperature connecting nucleate and transition regimes	[-]
Θ_{t-f}	knot temperature connecting transition and film regimes	[-]
λ	eigenvalue	[-]
ξ	$(z - v\tau)$ dimensionless co-ordinate	[-]
ρ	$(\hat{\rho}/\hat{\rho_{\mathrm{ref}}})$ reduced electrical resistivity	[-]
$\hat{\rho}$	electrical resistivity	[Ω m]
τ	dimensionless time	[-]
ϕ	$(\Phi/\Phi_{\mathrm{ref}})$ reduced electric potential	[-]
Φ	electric potential	[V]
Subscripts		
b	base $(x = 1)$	b
e	tip $(x = 0)$	e
LP	reference to limit points	LP
ref	reference value	ref
s	steady state	s
u	reference to uniform solutions	u
∞	ambient boiling liquid	∞
Superscripts		
$(')$	derivative with respect to x or to ξ	
Abbreviations		
CCP	Conduction-Convection Parameter	

References

1. Al'tov, V.A.; Zenkevich, V.B.; Kremlev, M.G.; Sychev, V.V. *Stabilization of Superconducting Magnetic Systems*; Plenum Press: New York, NY, USA, 1977.
2. Wilson, M.N. *Superconducting Magnets*; Oxford University Press: New York, NY, USA, 2002.
3. Yukikazu, I. *Case Studies in Superconducting Magnets. Design and Operational Issues*, 2nd ed.; Springer: New York, NY, USA, 2009.
4. Maddock, B.J.; James, G.B.; Norris, W.T. Superconductive composites: Heat transfer and steady state stabilization. *Cryogenics* **1969**, *9*, 261–273. [CrossRef]
5. Dresner, L. Propagation of normal zones in composite superconductors. *Cryogenics* **1976**, *16*, 675–681. [CrossRef]
6. Wilson, M.N.; Iwasa, Y. Stability of superconductors against localized disturbances of limited magnitude. *Cryogenics* **1978**, *18*, 17–25. [CrossRef]
7. Gurevich, A., VI; Mints, R.G. Self-heating in normal metals and superconductors. *Rev. Mod. Phys.* **1987**, *59*, 941–999. [CrossRef]
8. Bellis, R.H.; Iwasa, Y. Quench propagation in high T_c superconductors. *Cryogenics* **1994**, *34*, 129–144. [CrossRef]
9. Bottura, L. Modelling stability in superconducting cables. *Physica C* **1998**, *310*, 316–326. [CrossRef]
10. Yamamoto, E.T.; Watanabe, K.; Murase, S.; Nishijima, G.; Watanabe, K.; Kimura, A. Thermal stability of reinforced Nb_3Sn composite superconductor under cryocooled conditions. *Cryogenics* **2004**, *44*, 687–693. [CrossRef]
11. Vysotsky, V.S.; Sytnikov, V.E.; Rakhmanov, A.L.; Ilyin, Y. Analysis of stability and quench in HTS devices-New Approaches. *Fusion Eng. Des.* **2006**, *81*, 2417–2424. [CrossRef]
12. Martínez, E.; Young, E.A.; Bianchetti, M.; Muñoz, O.; Schlachter, S.I.; Yang, Y. Quench onset and propagation in Cu-stabilized multifilament MgB_2 conductors. *Supercond. Sci. Technol.* **2008**, *21*, 025009. [CrossRef]
13. Maeda, H.; Yanagisawa, Y. Recent developments in high temperature superconducting magnet technology. *IEEE Trans. Appl. Supercond.* **2014**, *24*, 4602412. [CrossRef]
14. Werweij, A.P. Thermal Runaway of the 13kA busbar joints in the LHC. *IEEE Trans. Appl. Supercond.* **2010**, *20*, 2155–2159. [CrossRef]
15. Willering, G.P.; Bottura, L.; Fessia, P.; Scheuerlein, C.; Werweij, A.P. Thermal Runaways in LHC interconnections: Experiments. *IEEE Trans. Appl. Supercond.* **2011**, *21*, 1781–1785. [CrossRef]
16. Rakhmanov, A.L.; Vysotsky, V.S.; Zmitrenko, N.V. Quench development in HTS objects—The possibility of "blow-up" regimes and a heat localization. *IEEE Trans. Appl. Supercond.* **2003**, *13*, 1942–1945. [CrossRef]
17. Romanovskii, V.R.; Watanabe, K. Operating modes of high-T_c composite superconductors and thermal runaway conditions under current charging. *Supercond. Sci. Technol.* **2006**, *19*, 541–550. [CrossRef]
18. Yanagisawa, Y.; Takizawa, A.; Hamada, M.; Nakagome, H.; Matsumoto, S.; Kiyoshi, T.; Suematsu, H.; Jin, X.; Takahashi, M.; Maeda, H. Suppression of catastrophic thermal runaway for a REBCO innermost coil of an LTS/REBCO NMR magnet operated at 400-600 MHz (9.4-14.1T). *IEEE Trans. Appl. Supercond.* **2014**, *24*, 4301005. [CrossRef]
19. Rocci, M.; Suri, D.; Kamra, A.; Vilela, G.; Nemes, N.M.; Martinez, J.L.; Hernandez, M.G.; Moodera, J.S. Large enhancement of critical current in superconducting devices by gate voltage. *Nano Lett.* **2020**, *21*, 216. [CrossRef] [PubMed]
20. Rocci, M. Gate-controlled suspended titanium nanobridge supercurrent transistor. *ACS Nano* **2020**, *14*, 12621–12628. [CrossRef]
21. Elmer, F.J. Limit cycles of the ballast resistors caused by intrinsic instabilities. *Z. Phys. B-Condens. Matter* **1992**, *87*, 377–386. [CrossRef]
22. Nukiyama, S. Maximum and minimum value of heat transmitted from a metal to boiling water under atmospheric pressure. *Int. J. Heat Mass Transfer* **1966**, *9*, 1419–1434. [CrossRef]
23. Zhukov, S.A.; Barelko, V.V.; Merzhanov, A.G. Wave Processes on Heat Generating Surfaces in Pool Boiling. *Int. J. Heat Mass Transfer* **1980**, *24*, 47–55. [CrossRef]
24. Zhukov, S.A.; Bokova, L.F.; Barelko, V.V. Certain Aspects of Autowave Transitions from Nucleate to Film Boiling Regimes with a Cylindrical Heat Generating Element Inclined from a Horizontal Position. *Int. J. Heat Mass Transfer* **1983**, *26*, 269–275. [CrossRef]
25. Zhukov, S.A.; Barelko, V.V. Nonuniform Steady States of the Boiling Process in the Transition Region between the Nucleate and Film Regimes. *Int. J. Heat Mass Transfer* **1983**, *26*, 1121–1130. [CrossRef]
26. Lee, D.J.; Lu, S.M. Two-mode boiling on a horizontal boiling wire. *AIChE J.* **1992**, *38*, 1115–1127. [CrossRef]
27. Nivoit, M.; Profizi, J.L.; Paulmier, D. Thermal equilibrium of a wire due to Joule heating. *Int. J. Heat Mass Transfer* **1981**, *24*, 707–713. [CrossRef]
28. Metaxas, A.C. *Foundations of Electroheat. A Unified Approach*; John Wiley & Sons: New York, NY, USA, 1996.
29. Speetjens, M.; Reusken, A.; Marquardt, W. Steady-state solutions in a nonlinear pool boiling model. *Commun. Nonlinear Sci. Numer. Simul.* **2008**, *13*, 1475–1494. [CrossRef]
30. Seydel, R. *Practical Bifurcation and Stability Analysis*, 3rd ed.; Springer: New York, NY, USA, 2009.
31. Witmer, G.; Balakotaih, V.; Luss, D. Finding singular points of two-point boundary value problems. *J. Comput. Phys.* **1986**, *65*, 244–250. [CrossRef]
32. Beyn, W.J. The numerical computation of connecting orbits in dynamical systems. *IMA J. Numer. Anal.* **1990**, *9*, 379–405. [CrossRef]
33. Friedman, M.J.; Doedel, E.J. Computational methods for global analysis of homoclinic and heteroclinic orbits: A case study. *J. Dyn. Differ. Equ.* **1993**, *5*, 37–57. [CrossRef]
34. Krikkis, R.N. On the multiple solutions of boiling fins with heat generation. *Int. J. Heat Mass Transfer* **2015**, *80*, 236–242. [CrossRef]

35. Krikkis, R.N. Laminar conjugate forced convection over a flat plate. Multiplicities and stability. *Int. J. Therm. Sci.* **2017**, *111*, 204–214. [CrossRef]
36. Kovalev, S.A.; Usatikov, S.V. Analysis of the Stability of Boiling Modes Involving the Use of Stability Diagrams. *High Temp.* **2003**, *41*, 68–78. [CrossRef]
37. Bantle, C.; Brunner, H. Blowup in diffusion equations: A survey. *J. Comput. Appl. Math.* **1998**, *97*, 3–22. [CrossRef]
38. Krikkis, R.N. Multiplicities and thermal runaway of current leads for superconducting magnets. *Cryogenics* **2017**, *83*, 8–16. [CrossRef]
39. Dabholkar, V.R.; Balakotaiah, V.; Luss, D. Travelling waves in multi-reaction systems. *Chem. Eng. Sci.* **1988**, *43*, 945–955. [CrossRef]
40. Bedeaux, D.; Mazur, P. Stability of inhomogeneous stationary states for the the hot-spot model of a superconducting microbridge. *Physica A* **1981**, *105*, 1–30. [CrossRef]
41. Luss, D.J.; Ervin, M.A. The influence of end effects on the behavior and stability of catalytic wires. *Chem. Eng. Sci.* **1972**, *27*, 315–327. [CrossRef]
42. Jackson, R. The stability of standing waves on a catalytic wire. *Chem. Eng. Sci.* **1972**, *27*, 2304–2306. [CrossRef]
43. Golubitsky, M.; Scaeffer, D. *Singularities and Groups in Bifurcation Theory*; Springer: New York, NY, USA, 1985; Volume 1–2.